High Rate Powder Deposition and Heat Transfer in Cold Spray

Presentation: Dr. Ozan Ozdemir
Cold Spray Action Team Meeting
Worcester Polytechnic Institute, Worcester, MA
June 19-20, 2018

Team

Northeastern University	Army Research Laboratory	United Technologies Research Center	VRC Metal Systems
Dr. Ozan Ozdemir Dr. Sinan Muftu Dr. Teiichi Ando Qiyong Chen Lauren Randaccio Tricia Schwartz	Vic Champagne Aaron Nardi	Dr. Matt Siopis	Kiley Plooster Kris Klus Terree Matson Rob Hrabe Robert Allegretto

Cold Spray

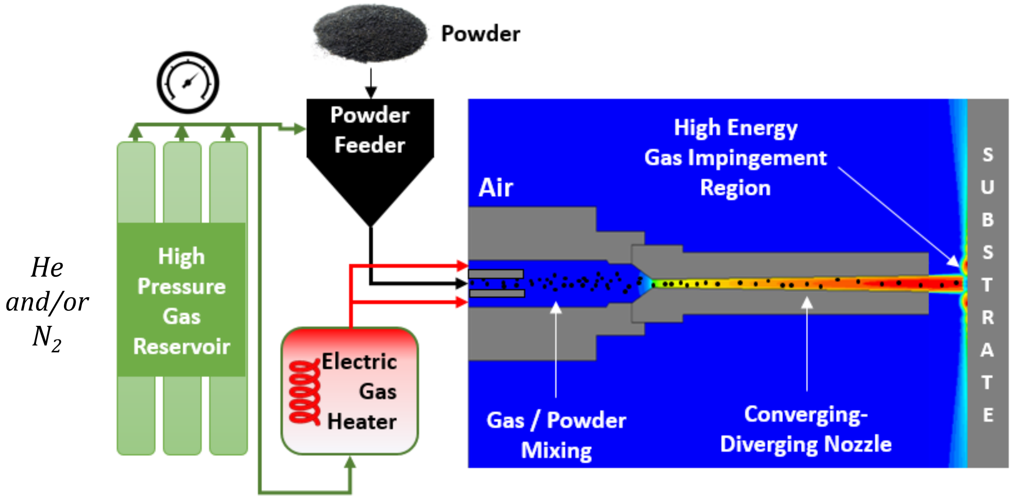

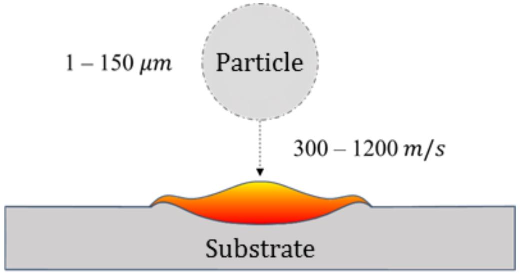

Materials

Predominantly metals, but ceramics, polymers, composites, and dissimilar materials have been successfully demonstrated.

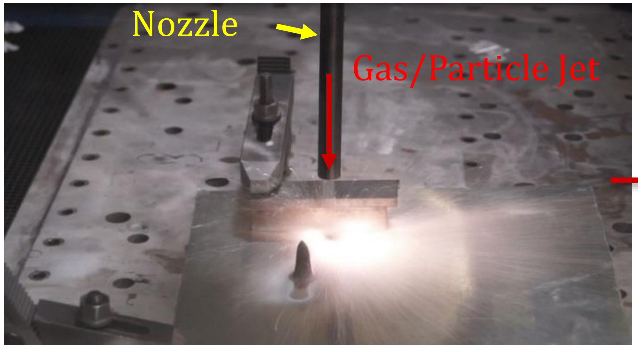

Spray Process

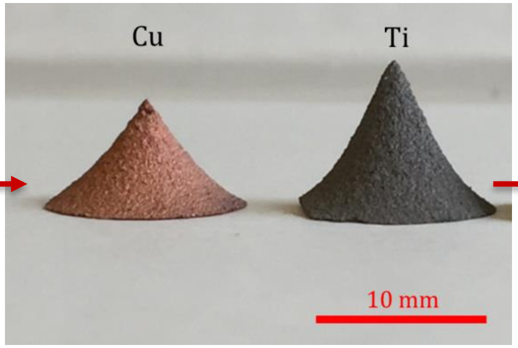

Deposition Process

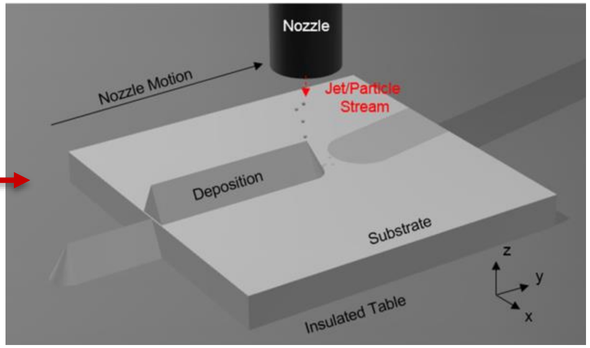

Building Process

Generating Coatings and Components

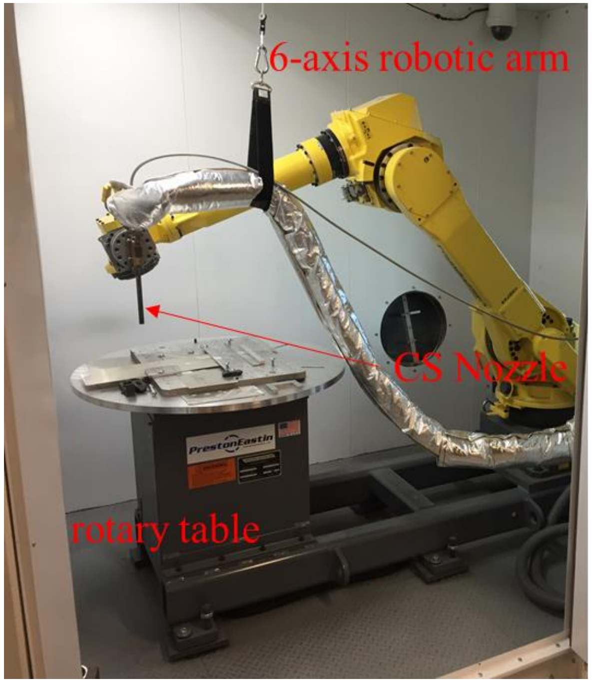

NU CS Laboratory

- Coatings
- Repair of Components
- Additive/Subtractive Manufacturing of Components
- 3D Printing

Transitioning CS into a Manufacturing Process

- How fast can I produce a component with CS?
  - Decrease cost and conserve materials
- If I build the component in 1 hour versus 3 hours;
  - How is structural integrity affected?
  - How much heat is the component experiencing?
  - Are there any major changes to adhesion properties?
  - Are there any major changes to the microstructure?

Discussion Points

1. Understanding and maximizing build speed by increasing powder deposition rates
    i. Cost
    ii. Turnaround time
    iii. Conservation of consumables and nonrenewable resources
2. Understanding heat generation and controlling thermal input
    i. Application for thermally sensitive components
    ii. Controlling thermally added stresses

Cold Spray Process & Increasing Powder Deposition Rates

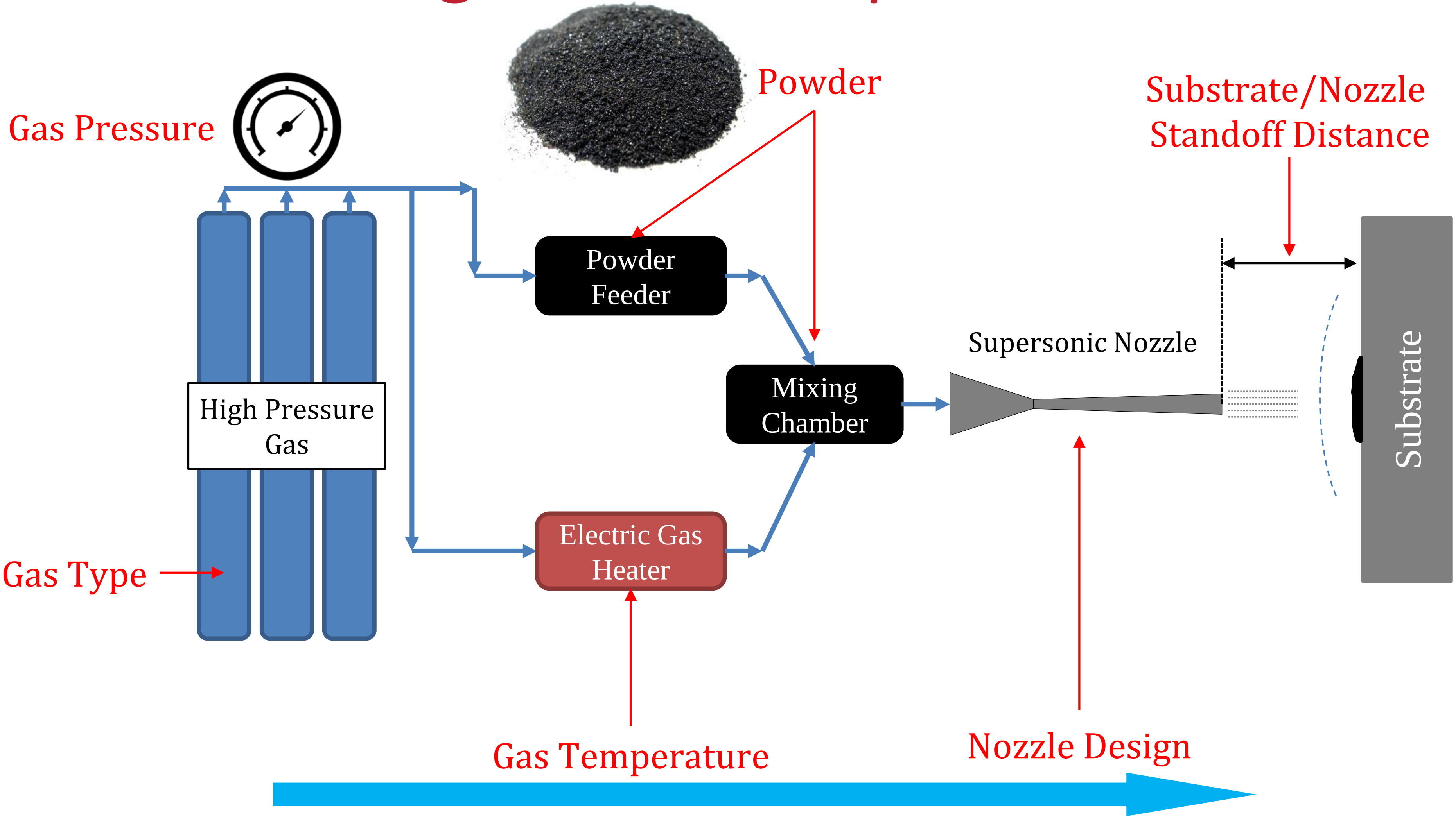

MANY VARIABLES

Bonding Mechanism & Criteria

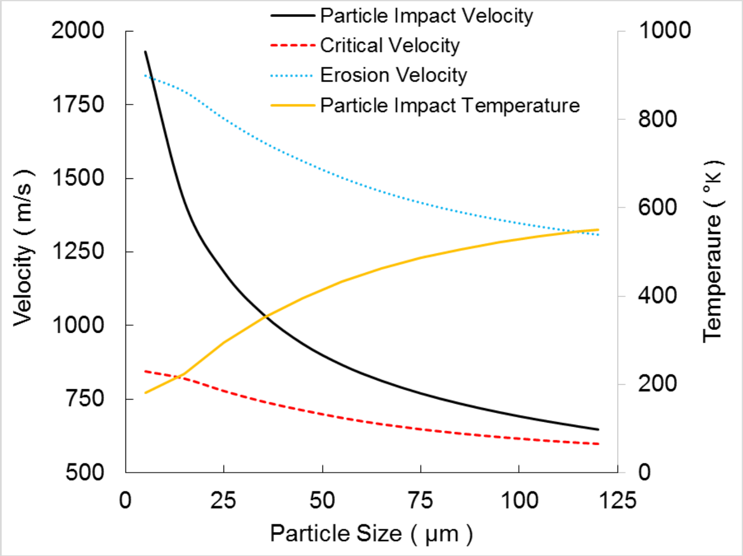

$$u_{cr/er} = \sqrt{\frac{4C_1\,\sigma_{ult}}{\rho_p}\left(1-\frac{T_{pi}-T_r}{T_m-T_r}\right) + C_2\, c_{p_p}\,(T_m - T_{pi})}$$

Fitting Constants

Erosion Velocity

$C_1 = 1.2$ $C_2 = 0.8$

Critical Velocity

$C_1 = 4.8$ $C_2 = 1.2$

Assadi et al. (2003)
Schmidt et al. (2006)
Schmidt et al. (2009)
Assadi et al. (2013)

CS Modeling Team

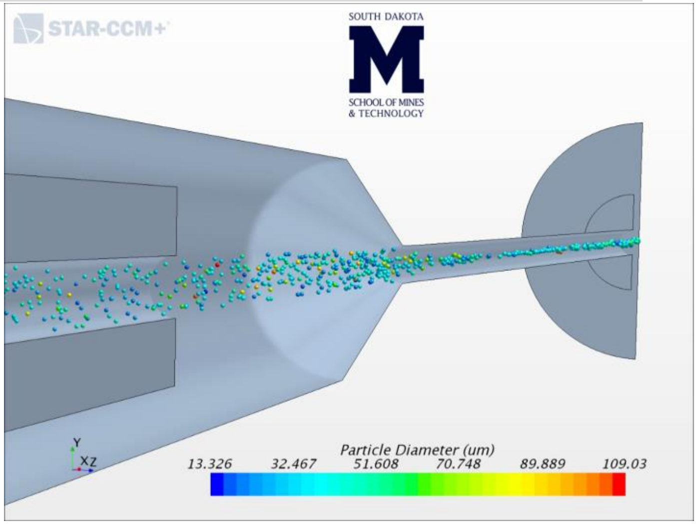

O. Ozdemir, C. Widener, SDSM&T

experiments

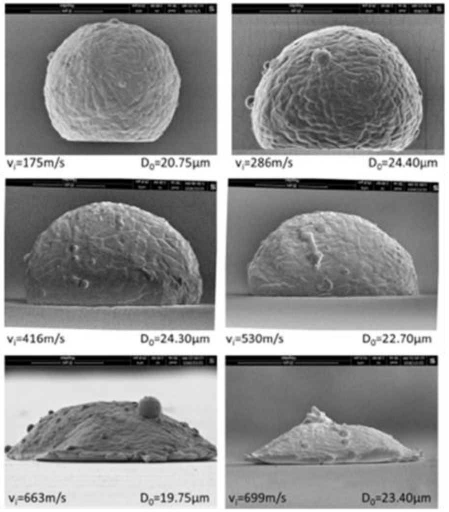

W. Xie, J.-H. Lee, UMASS

model results

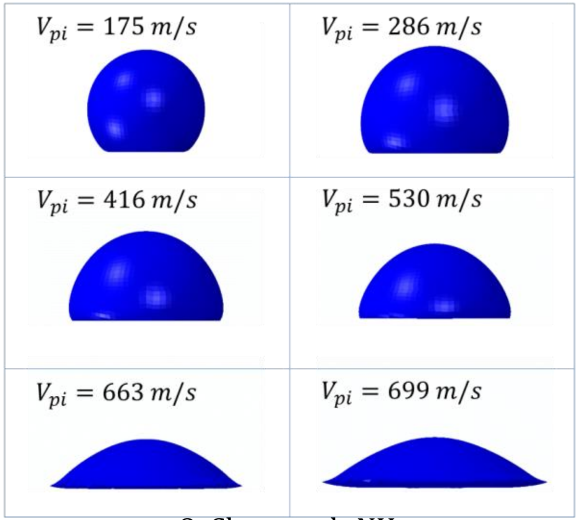

Q. Chen, et al., NU

η (or CVR) value & Deposition Efficiency

$$\eta = \frac{Particle\ Impact\ Velocity}{Critical\ Velocity}$$

$$DE(\%) = 100 \times \frac{Mass\ of\ Bonding\ Particles}{Mass\ of\ Sprayed\ Particles}$$

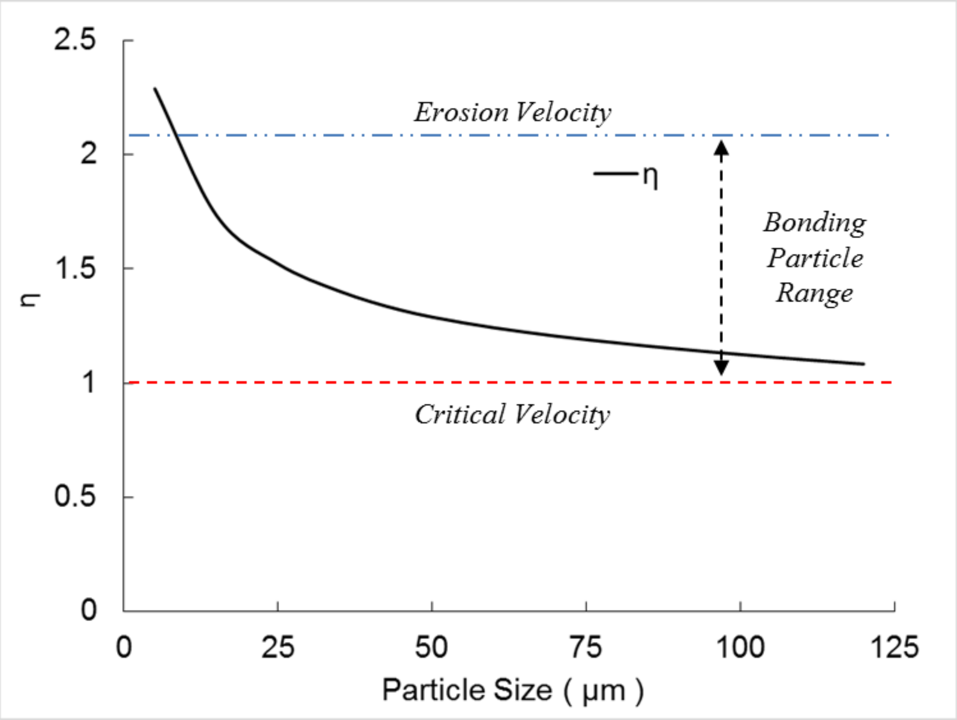

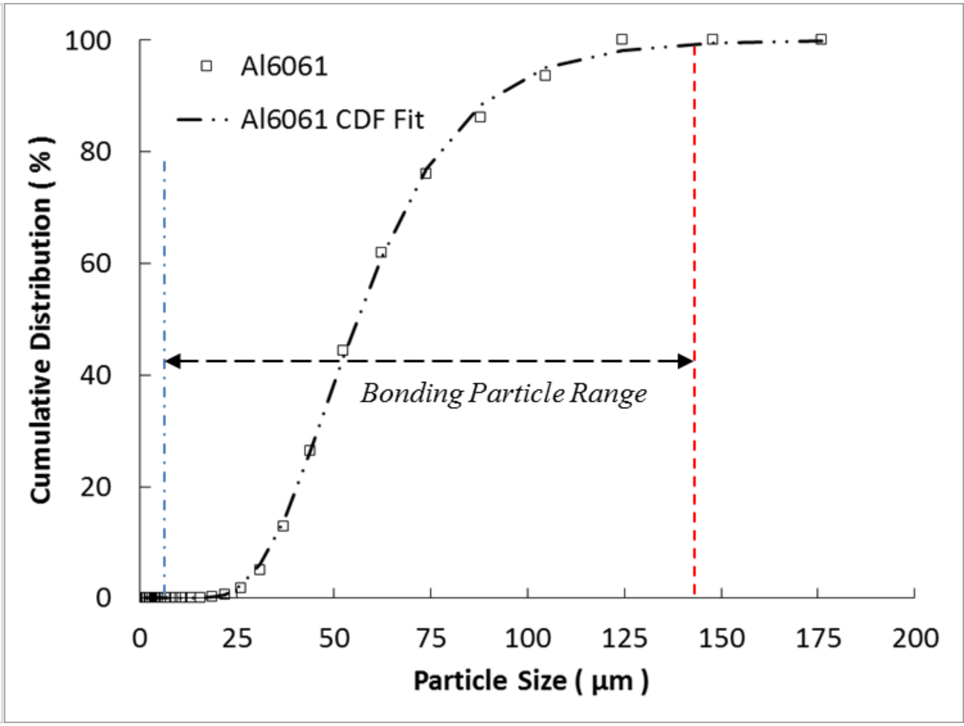

In the Supersonic Nozzle

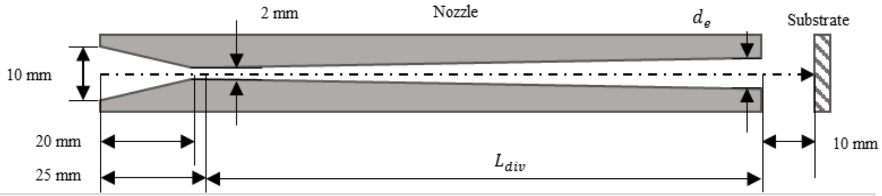

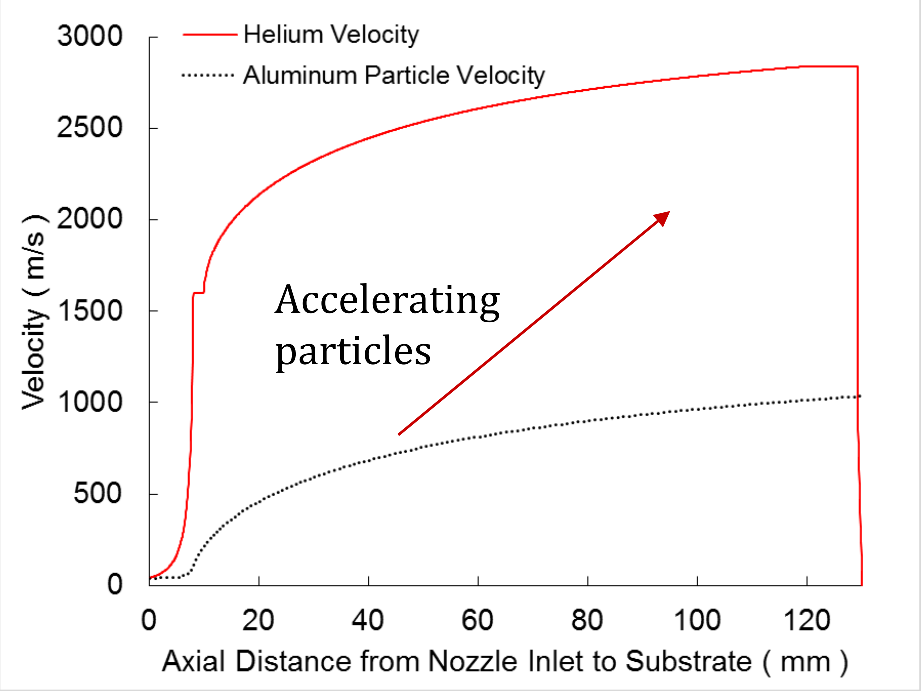

Accelerating particles

Particle drag generated by gas-particle velocity difference

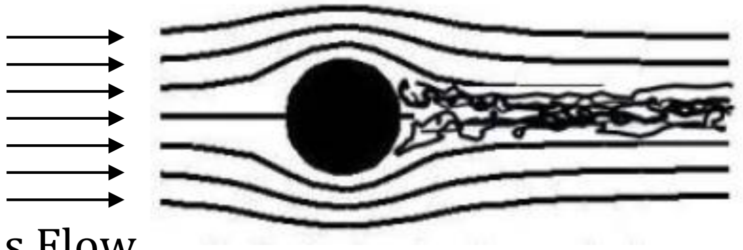

Gas Flow

Image Source: https://www.grc.nasa.gov/www/k-12/airplane/dragsphere.html

Gas Capacity

- Thrust (force) available in nozzle
  - $Thrust = Gas\ mass\ flow\ rate \times Gas\ Velocity$

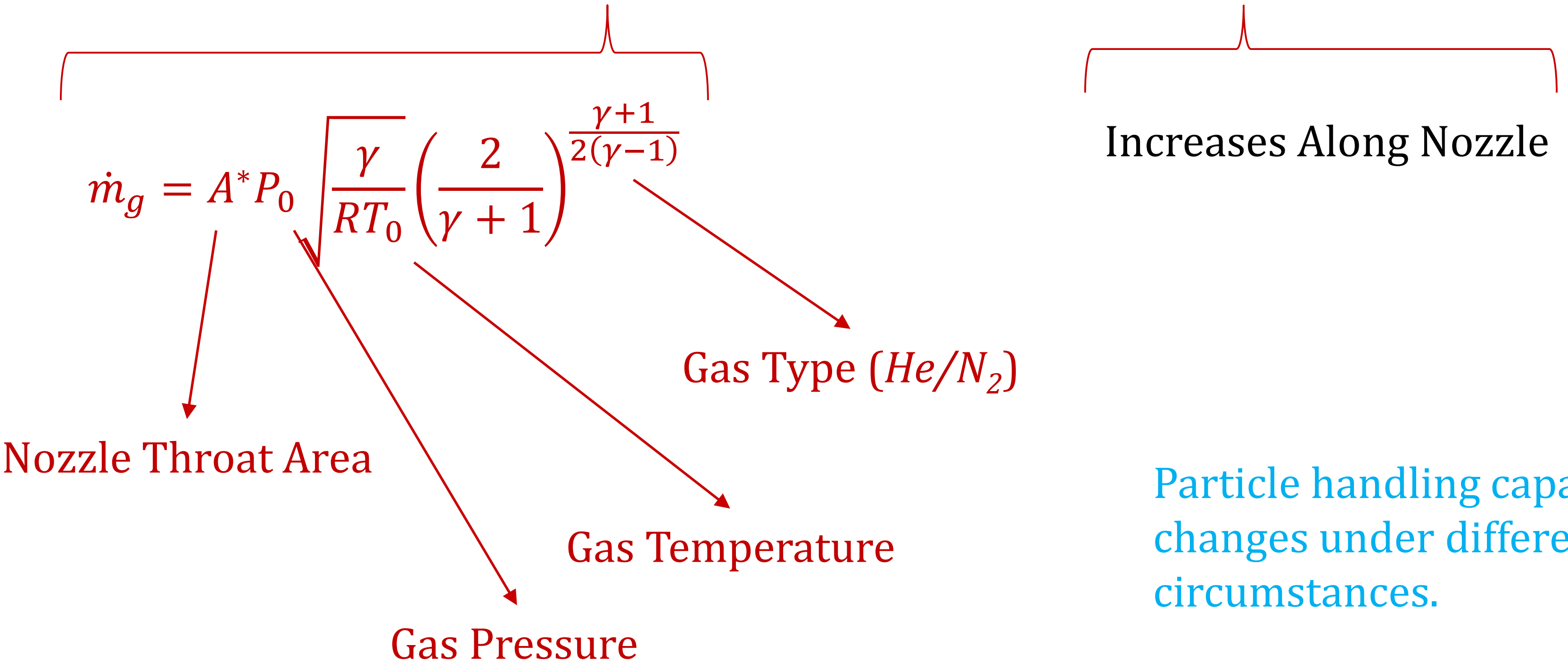

$$\dot{m}_g = A^* P_0 \sqrt{\frac{\gamma}{RT_0}} \left(\frac{2}{\gamma+1}\right)^{\frac{\gamma+1}{2(\gamma-1)}}$$

Nozzle Throat Area

Gas Pressure

Gas Temperature

Gas Type (He/N_2)

Increases Along Nozzle

Particle handling capacity changes under different circumstances.

Particle Stream Loading Rate

$$Particle\ Loading\ Rate(\%) = 100 \times \frac{Particle\ Feed\ Rate\ \left(\frac{kg}{s}\right)}{Gas\ Flow\ Rate\ \left(\frac{kg}{s}\right)}$$

Maximize this parameter for highest gas usage efficiency

Increasing this parameter reduces particle impact velocity

How much reduction? What are physical limitations?

Powder Feeding Capacity & Limitations

- Traditionally:
  - < 15 g/min (1,2,3)
  - < 5% wt. of gas
- New information:
  - Higher feed rates possible(4)

Need

- Comprehensive understanding of powder feeding capacity and limitations.

Importance

- More deposition per volume of gas spent
  - Maximize deposition speed
    - Reduce cost / part

1. Taylor et al. (2005)
2. Champagne (2008)
3. Schmidt et al. (2009)
4. Meyer et al. (2016)

Gas Dynamic Model for Handling Powder Loading Losses

Build Two-way Coupled Quasi-1D Model

Continuity

$$\frac{\partial}{\partial t}\oiiint \rho\, dV + \oiint \rho\, \boldsymbol{u}\cdot \boldsymbol{dS} = 0$$

Momentum

$$\frac{\partial}{\partial t}\oiiint (\rho u)\, dV + \oiint (\rho u \boldsymbol{u})\cdot \boldsymbol{dS} = -\oiint (p\, dS)_x + \boldsymbol{F}_p$$

Energy

$$\frac{\partial}{\partial t}\oiiint \rho\left(e+\frac{u^2}{2}\right) dV + \oiint \rho\left(e+\frac{u^2}{2}\right)\boldsymbol{u}\cdot\boldsymbol{dS} = -\oiint (p\boldsymbol{u})\cdot\boldsymbol{dS} + \dot{Q}_p + \boldsymbol{F}_p\cdot\boldsymbol{u}_p$$

Study Particle Loading Effects on Aerodynamics

Numerical Tests (~5800 Simulations)

Useful for Optimization

Numerical models show minimal effects on particle impact conditions with increase in particle loading rate.

Other Materials

Traditional Range of Deposition
0-15 g/min
aluminum generally < 5 g/min

Loss in Eta (%)

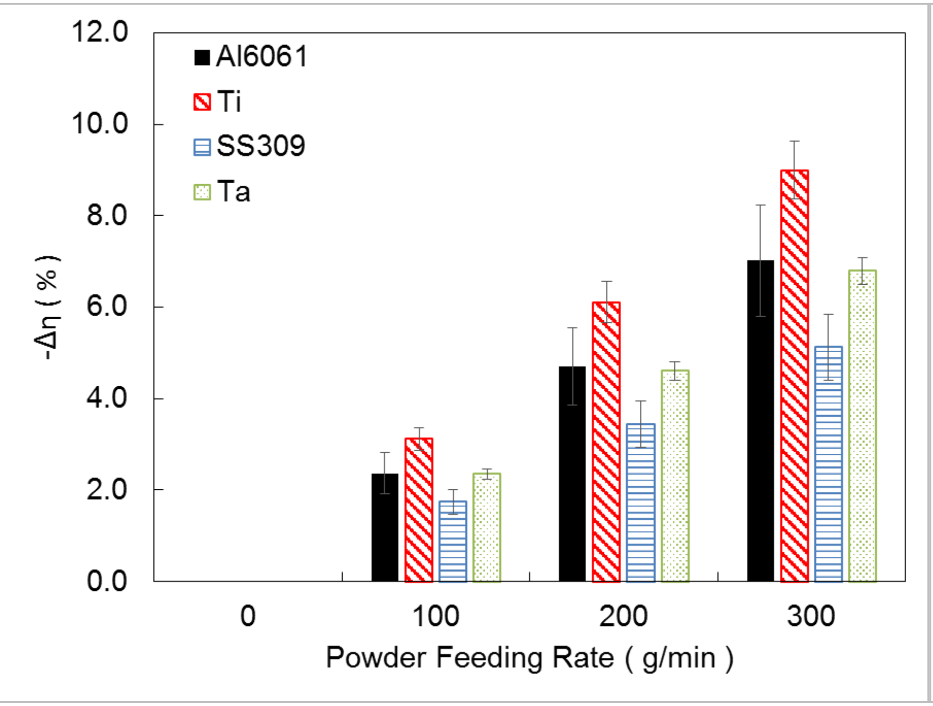

Deposition Efficiency (%)

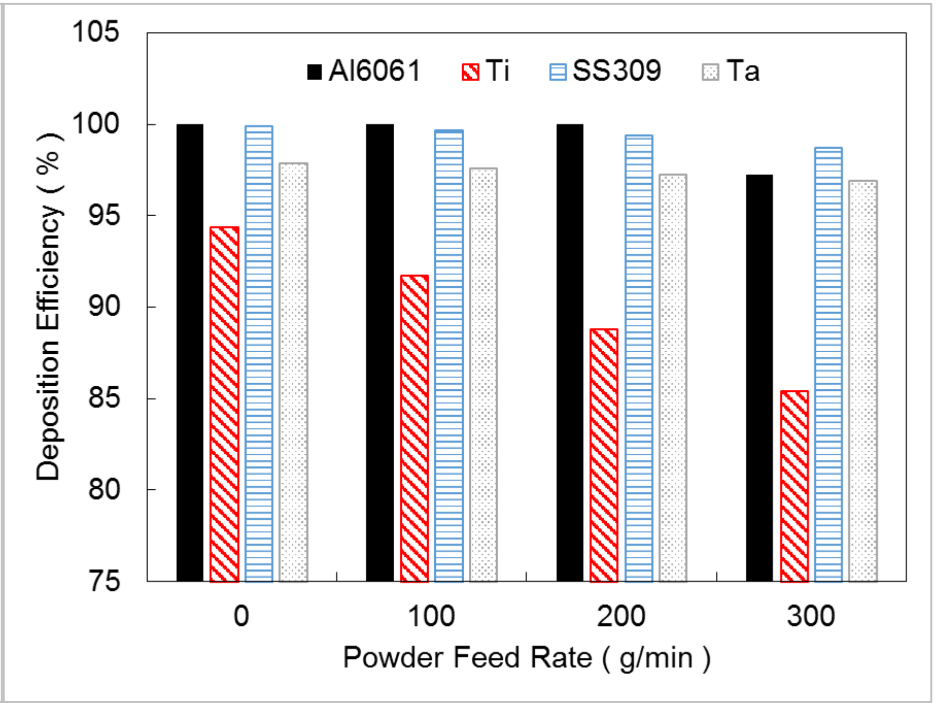

Fluid stream loading: 0 – 60% Particles in Gas Stream by weight

High Speed Deposition Limitations

Major limiting factors
- Traverse robot speeds
- Residual stress management
- Safety management

Buildup Desired = 0.25 mm/layer
V_{nozzle} = 612 mm/s

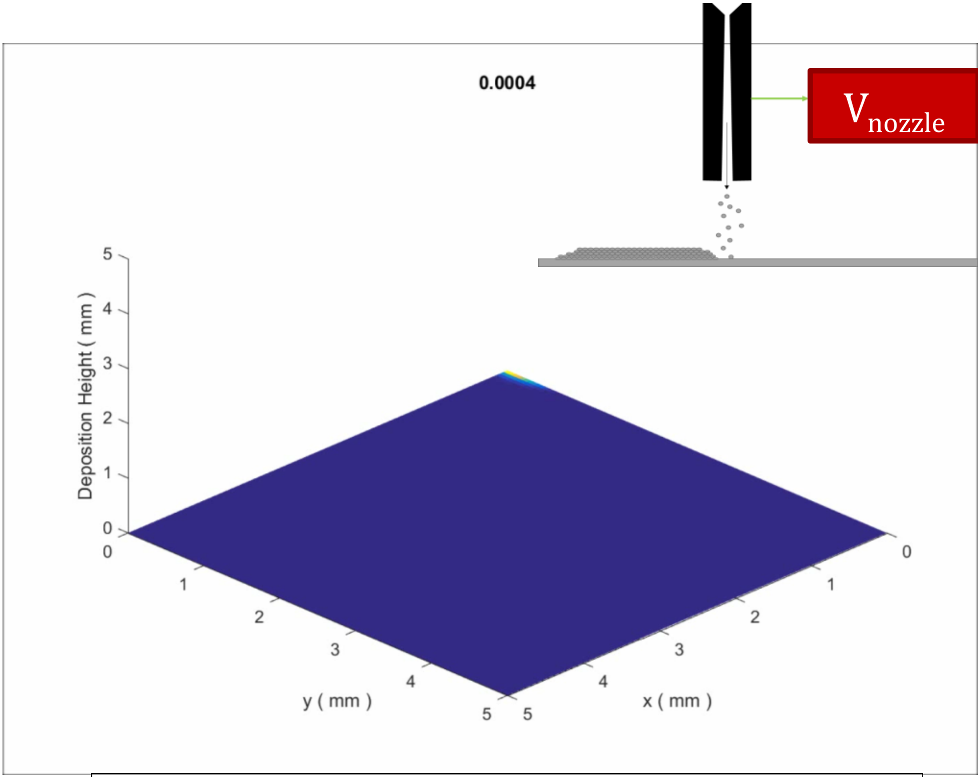

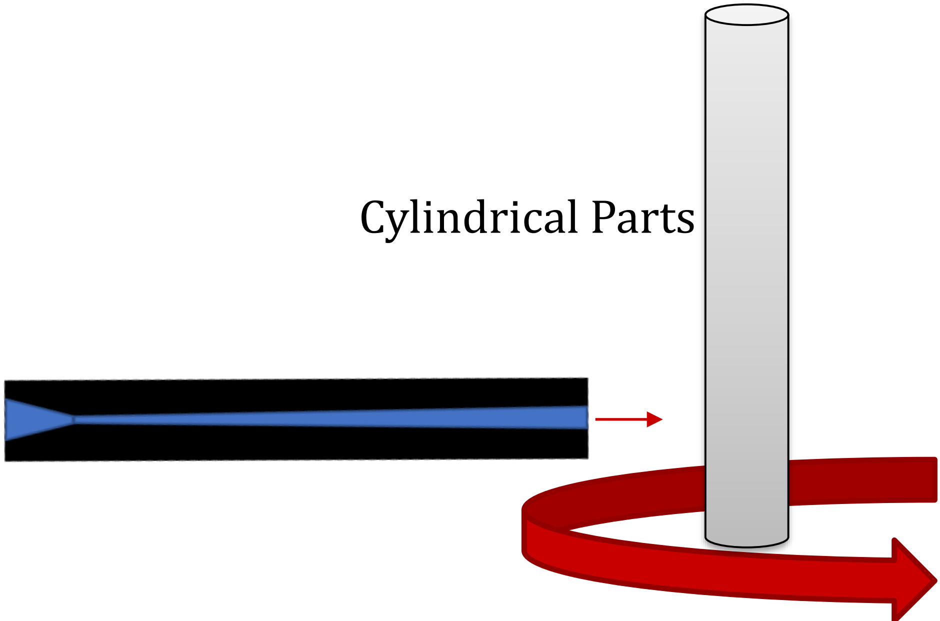

Powder Feed Rate	13.66 g/min
Powder Density	2700 kg/m^3
Volumetric Buildup Rate	84.32 mm^3/s

Case Study: Tantalum

Study

- Vary particle loading
  - 5% to 15%
  - 1.6 kg/hr to 4.7 kg/hr
  - Triple speed and observe mechanical and microstructural effects
- Samples placed on a cylindrical fixture
- Tantalum on hardened 4140 steel

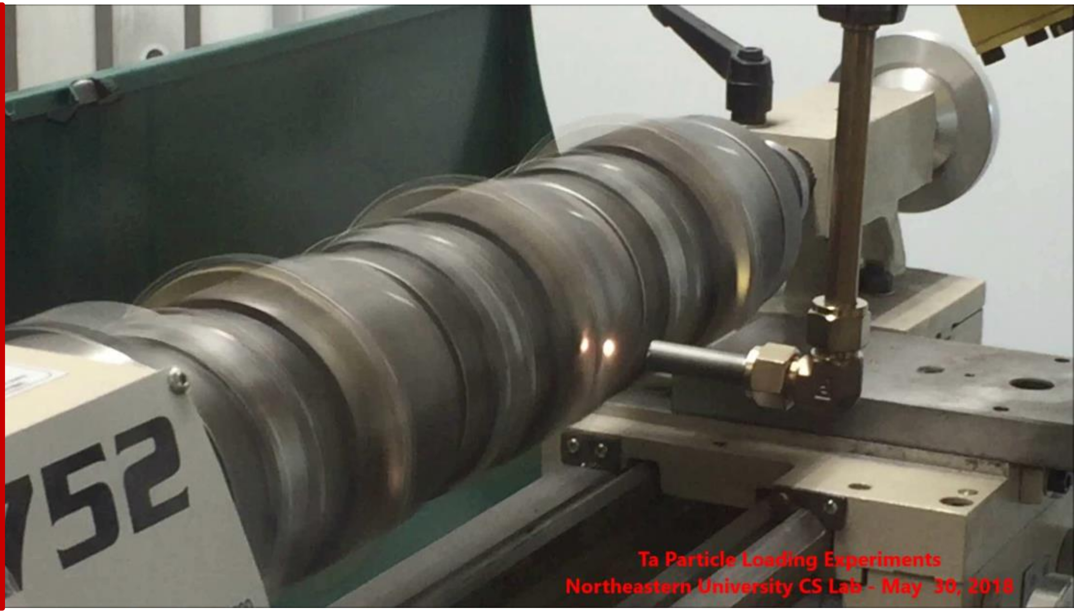

Ta Particle Loading Experiments
Northeastern University CS Lab - May 30, 2018

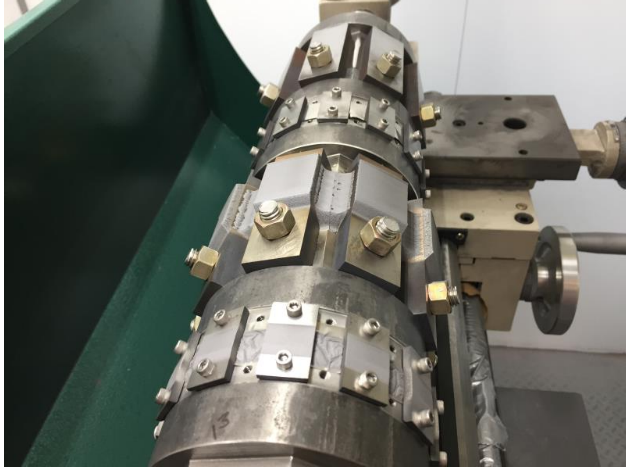

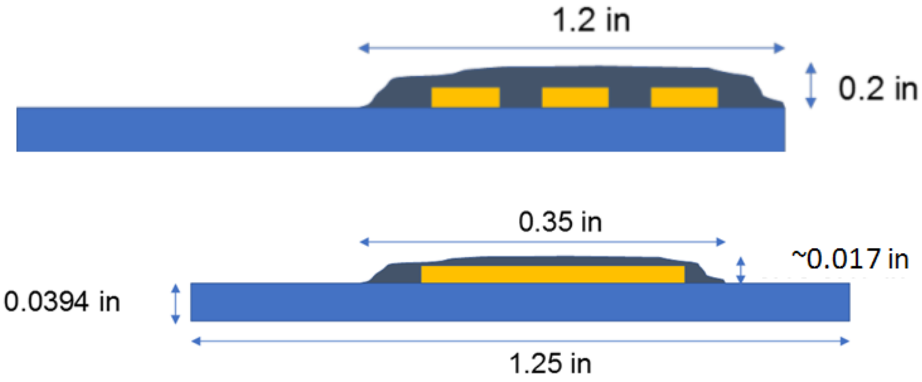

Effects on Impact Velocity

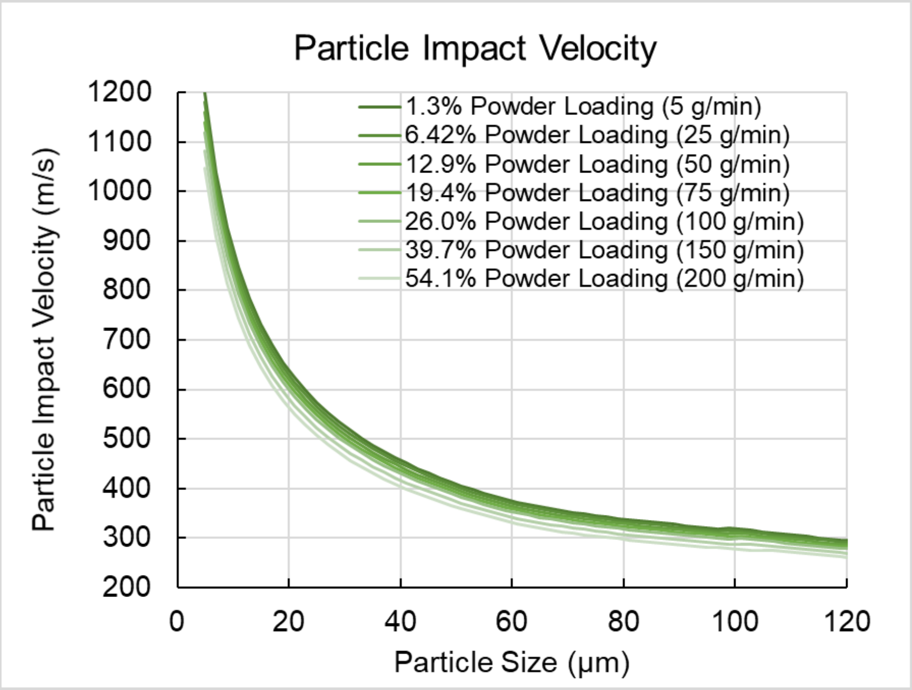

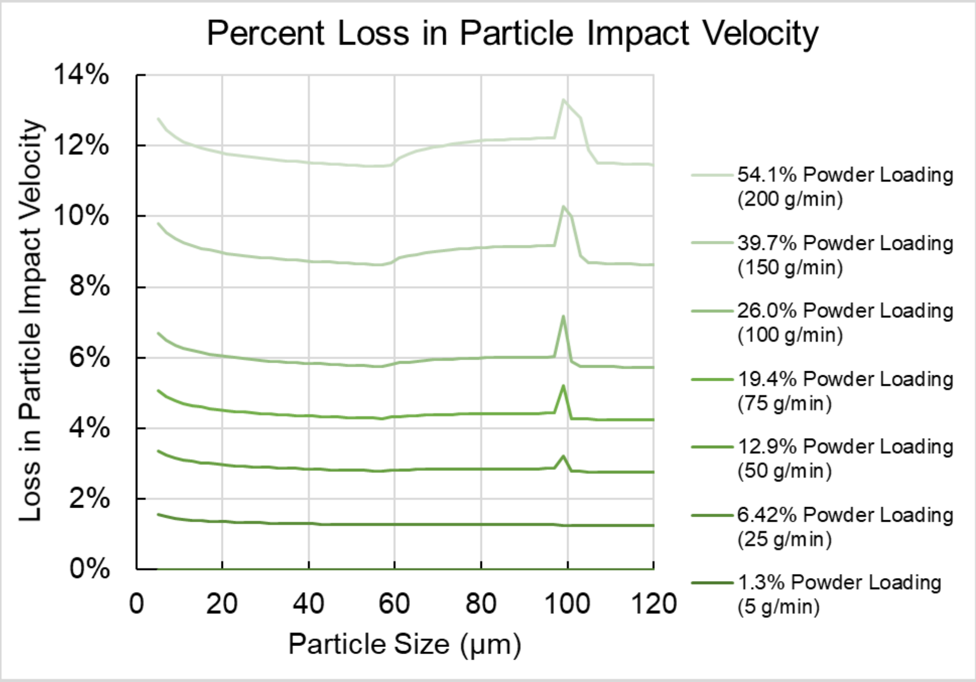

Effects on Critical Velocity Ratio (η)

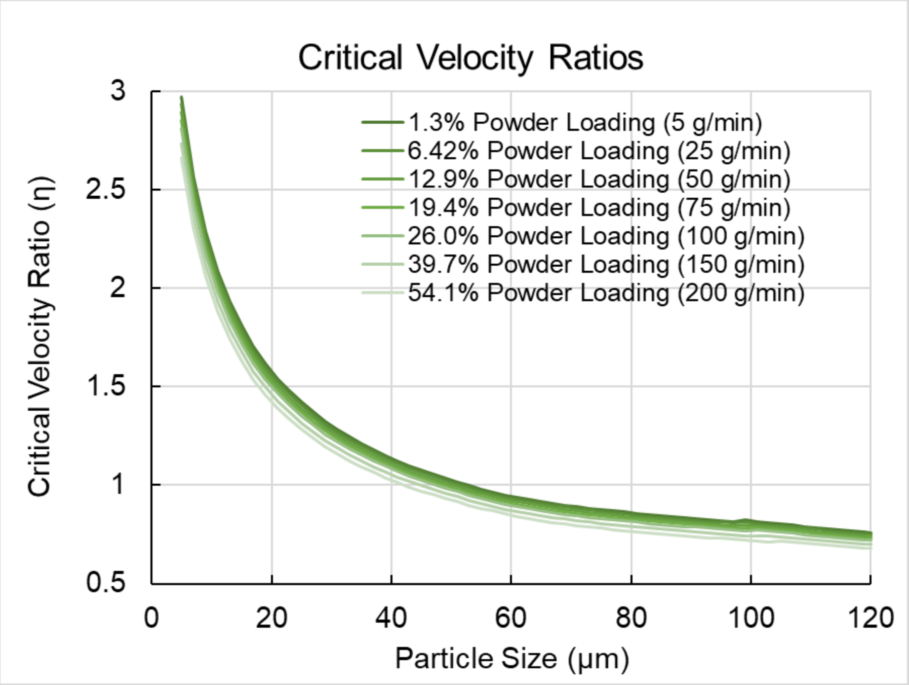

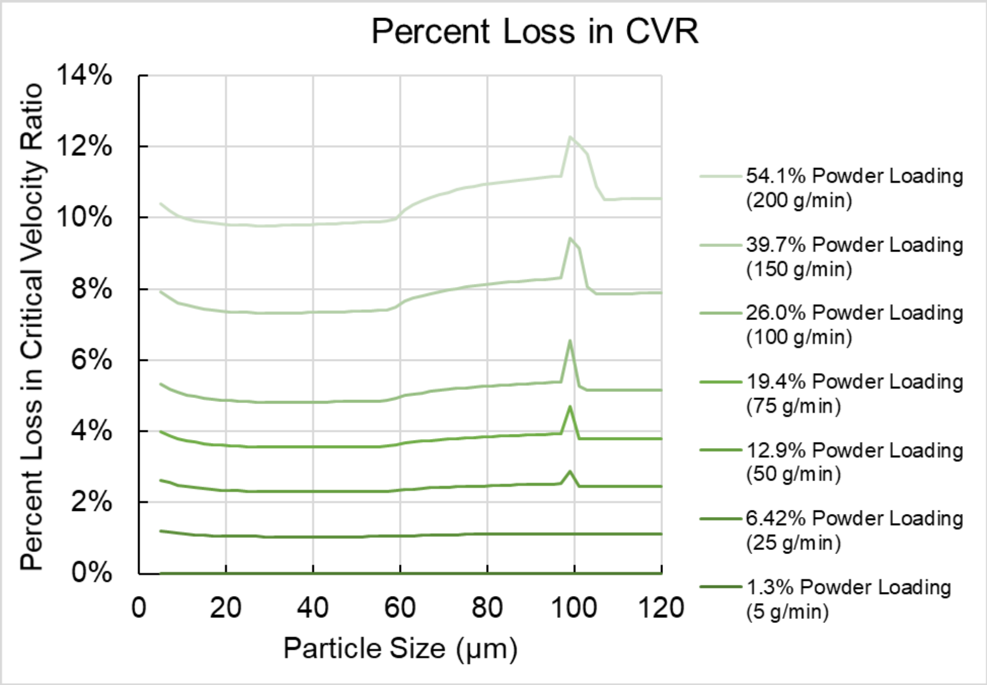

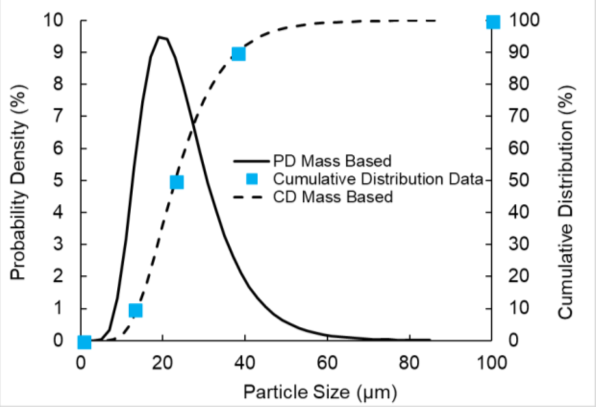

Microstructure Comparison

8 layers
0.49 mm
0.0194”

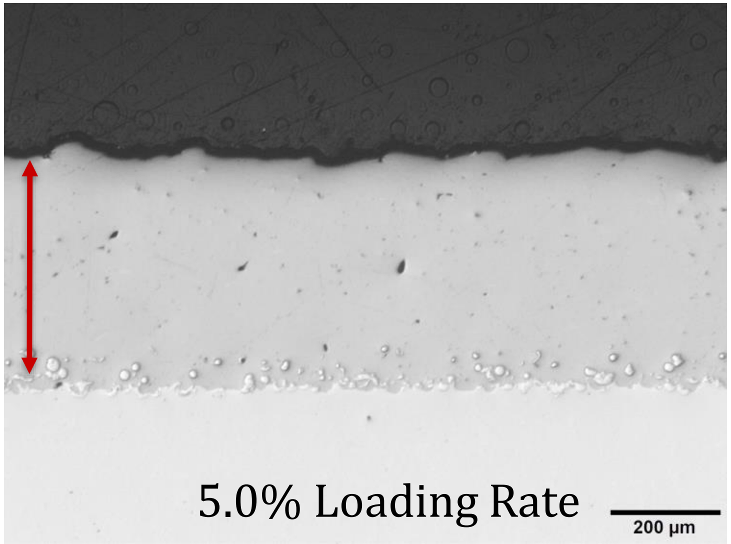

6 layers
0.39 mm
0.0155”

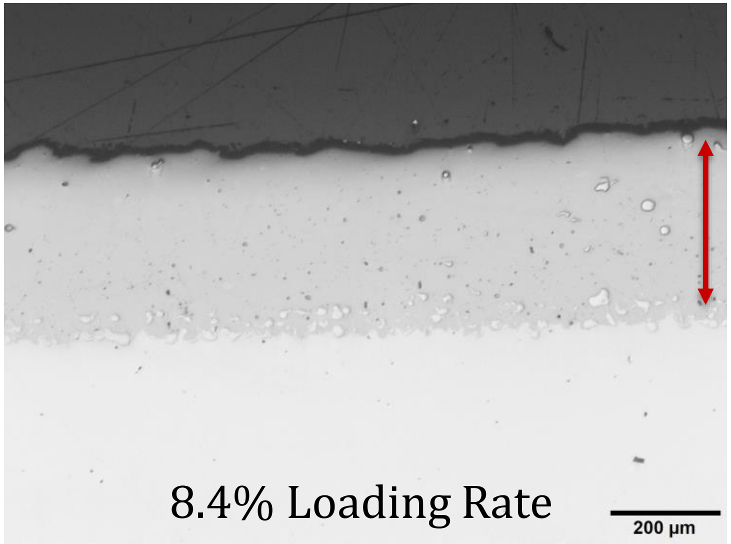

8 layers
0.62 mm
0.0243”

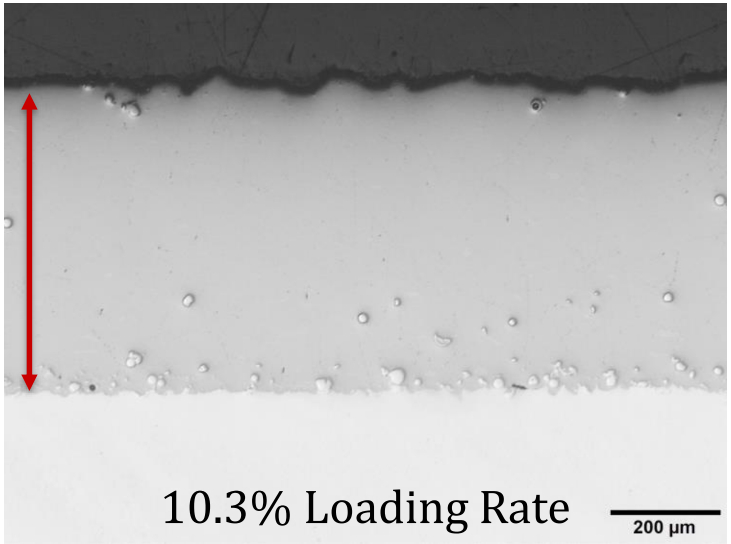

8 layers
0.52 mm
0.0205”

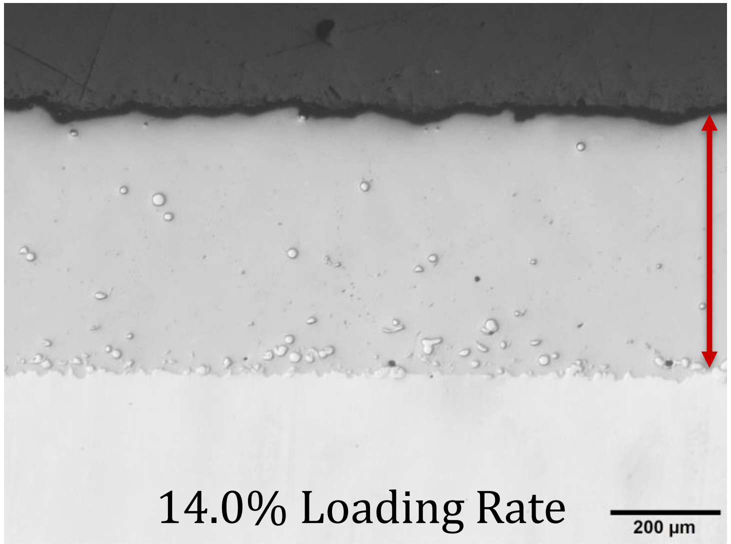

Microhardness Comparison

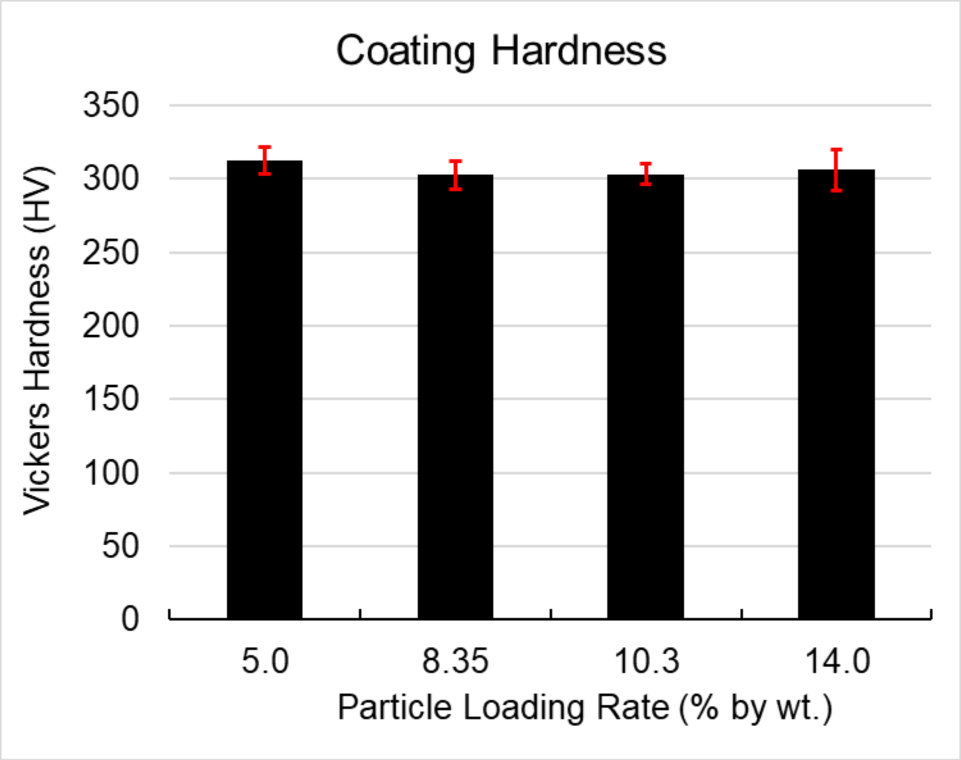

No statistical evidence to show that the means of the data sets are different.

$300\ HV \approx 30\ HRC$

Adhesive Strength (Three-Lug Shear Test)

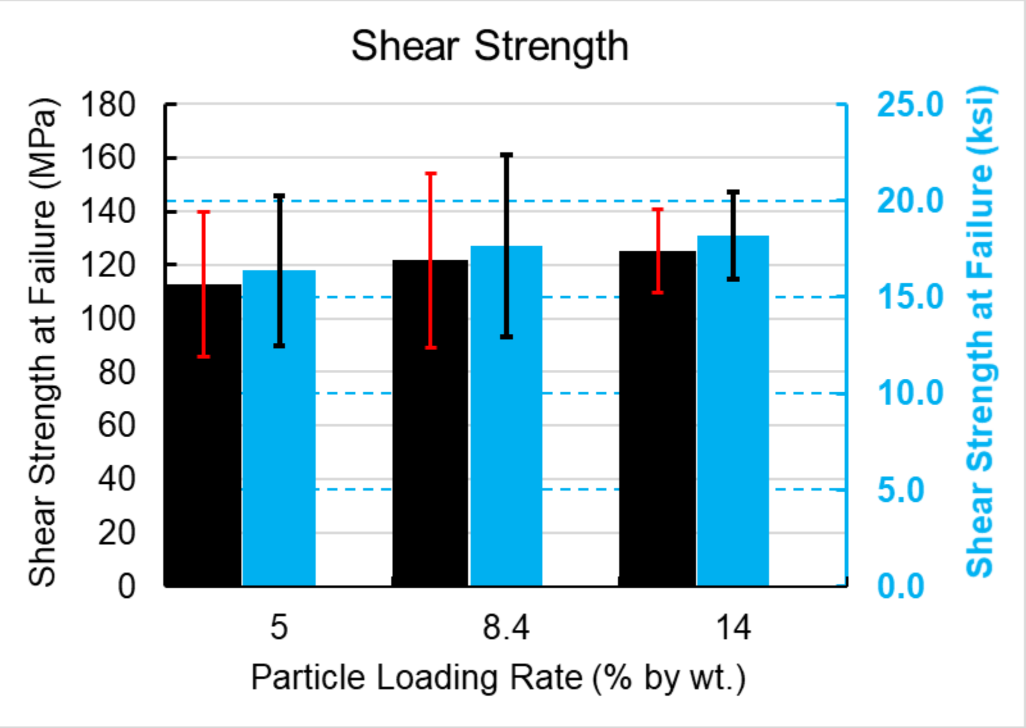

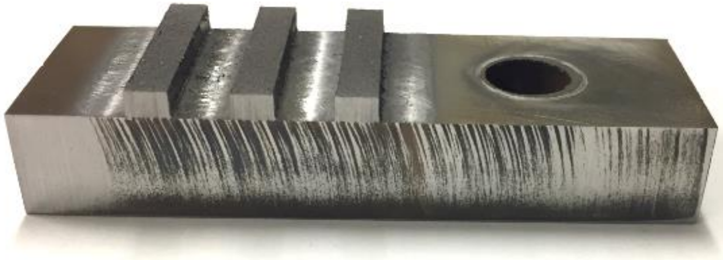

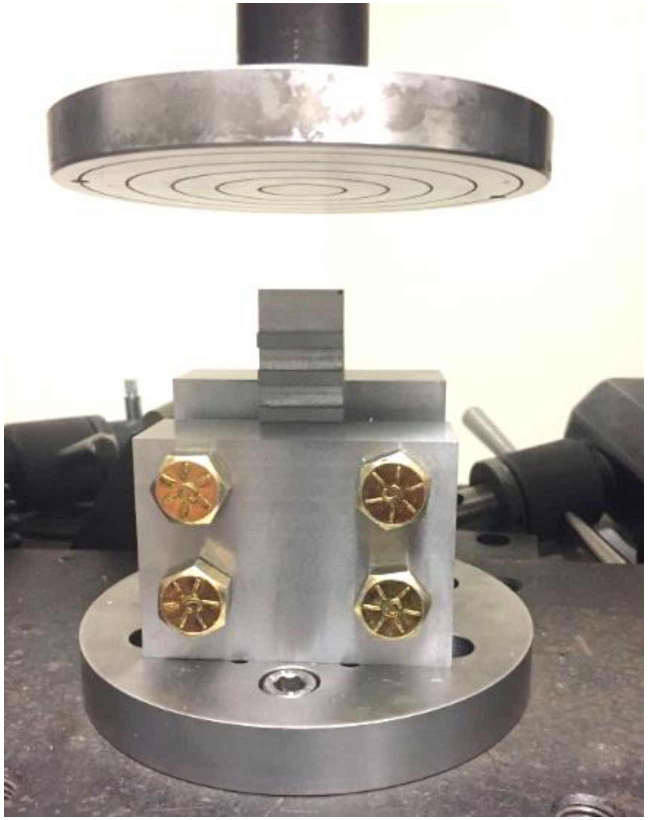

No statistical evidence to show that the means of the data sets are different.

Stress Related Coating Delamination

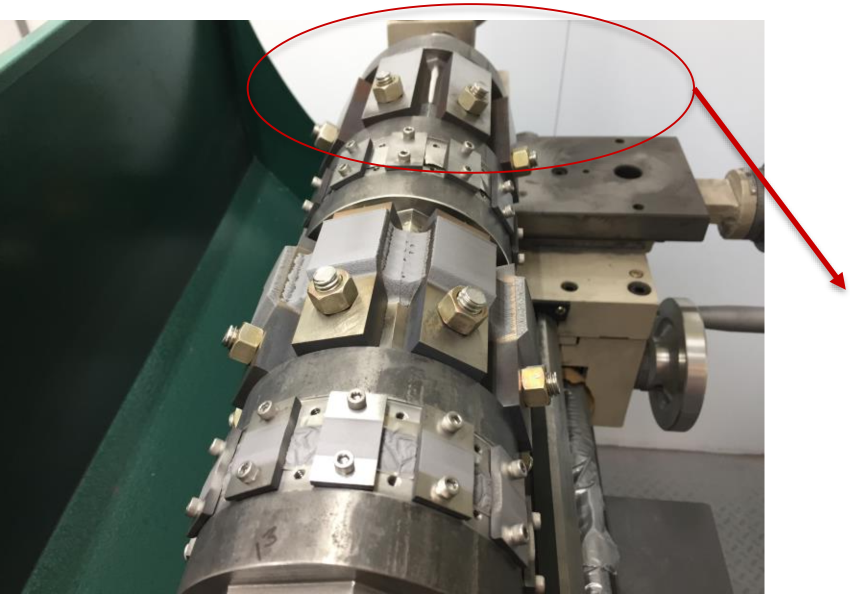

Observations related to coating detachment

- When building thick specimens.
- Coating detachment observed for large samples 5.0%, 8.3%, 10.4% (all) loading rates.
- No delamination observed for 14% loading rate.
- Delamination observed after lathe was left running for ~10 mins after run.
- Detachment not observed for large small specimens. (thin layered coating)

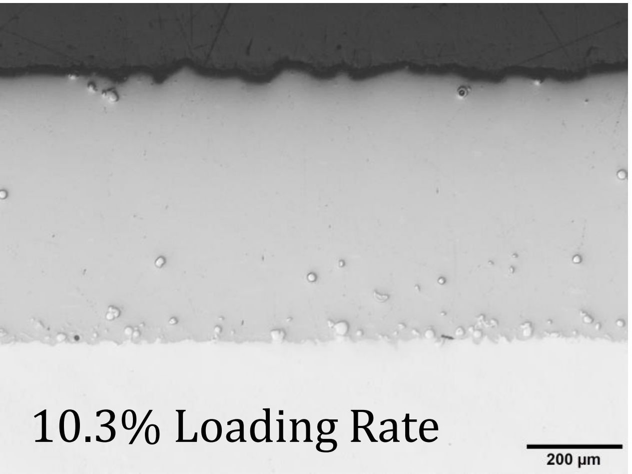

10.3% Loading Rate

Tantalum - CTE	~6.50 µm/m-°C
4140 Steel - CTE	~12.2 µm/m-°C

Conclusions

1. High rate deposition is ideal for cylindrical components
2. Cost, time, materials savings can easily be tripled compared to current practices.
3. No negative mechanical and microstructural effects are currently correlated to deposition rate increase.
4. Work is needed in thick coating stress control via thermal control

Gas Cost per kg of Deposition
($/kg)

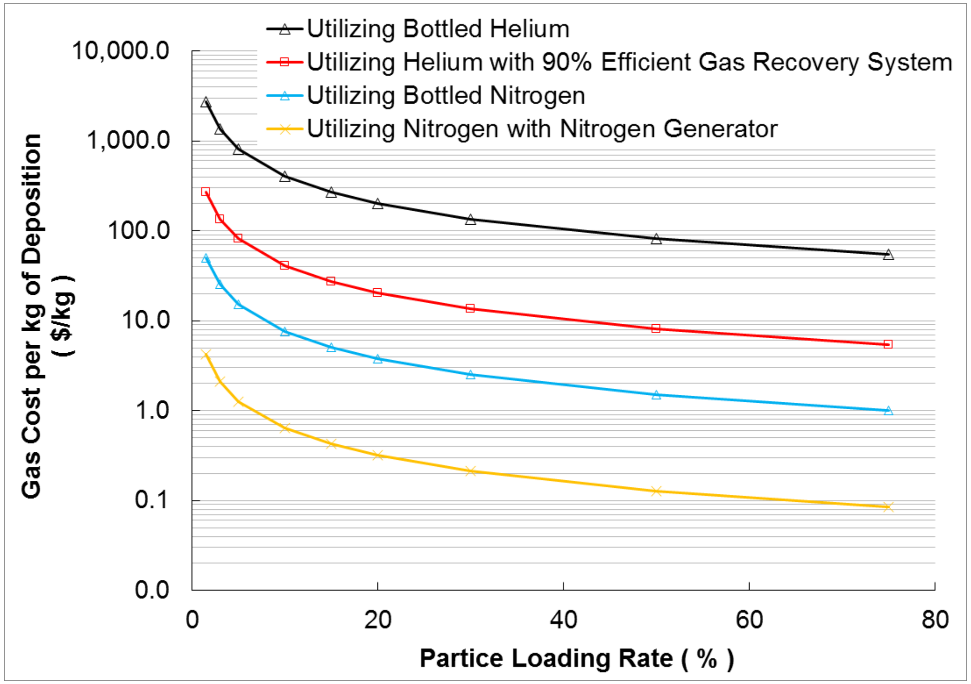

Cost of Helium	7.27	$\$/\mathrm{m}^3$
	41.00	$/kg
Cost of N2	1.00	$\$/\mathrm{m}^3$
	0.76	$/kg

U.S. Geological Survey, Mineral Commodity Summaries, January 2016

Prepared by John E. Hamak7 [(806) 356–1031, jhamak@blm.gov]

http://www.glair.com/GN2/GN2_Main.htm

Noncylindrical Geometries Powder Loading Optimization (maximization)

1. Adjust powder feeding rate to control loading rate
    1. Deposition speed
    2. Mass production
    3. Longer sprays to cover large areas
    4. Cost savings
    5. Conservation of helium

2. Adjust nozzle throat size
    1. Reached max feed rate
    2. Longer sprays to cover large areas
    3. Cost savings
    4. Efficient use of helium

Nozzle Powder Loading Capacity

Pressure: 40 bars (580 psi)
Temperature: 500 °C (932 °F)

$$Particle\ Loading\ Rate(\%) = 100 \times \frac{Particle\ Feed\ Rate\ \left(\frac{kg}{s}\right)}{Gas\ Flow\ Rate\ \left(\frac{kg}{s}\right)}$$

In Nitrogen

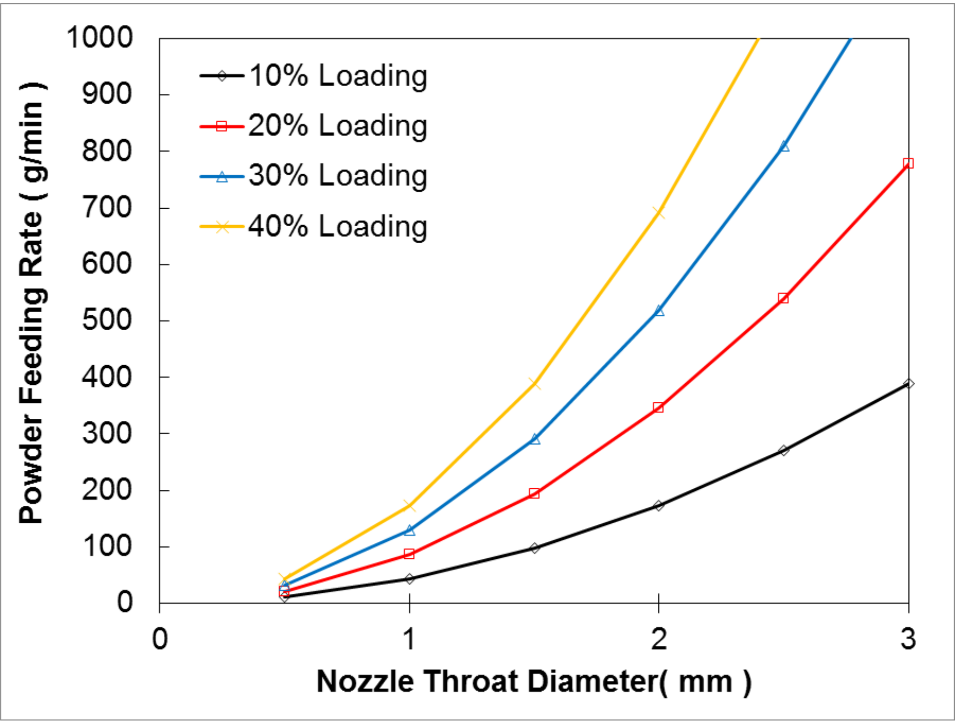

In Helium

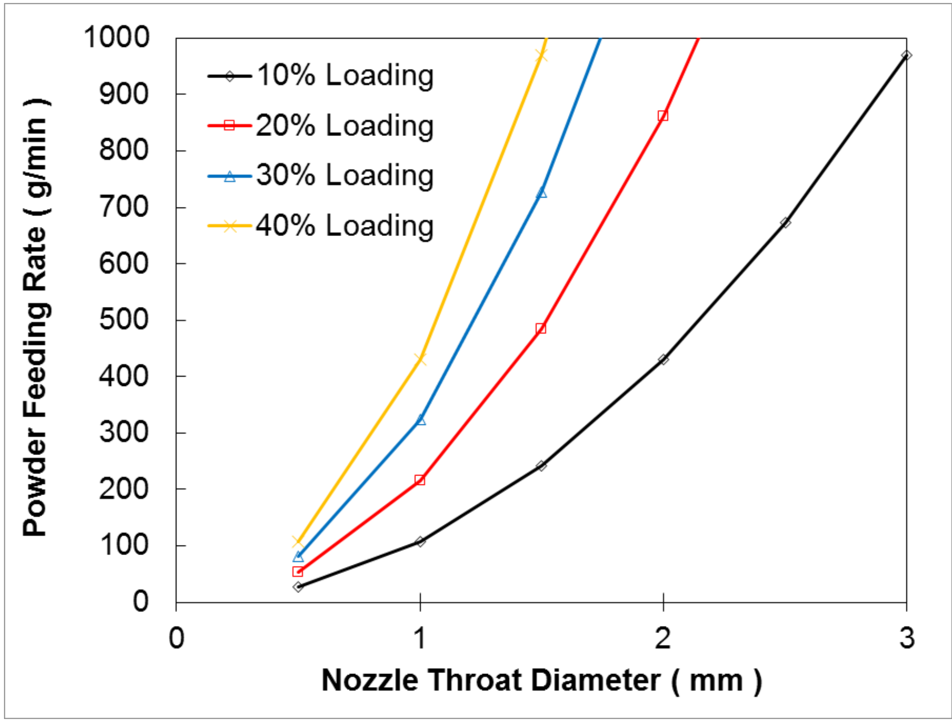

Heat Generation in Cold Spray

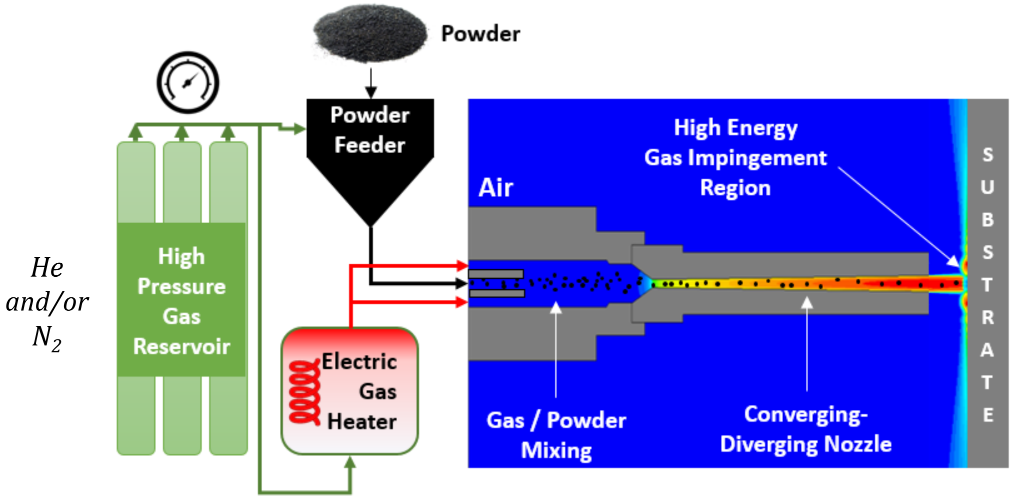

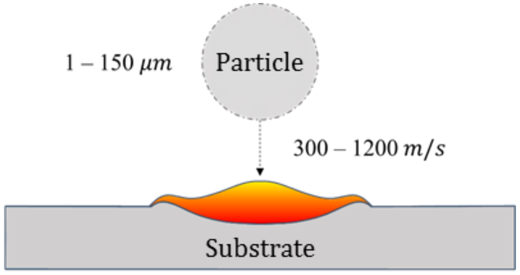

Materials

Predominantly metals, but ceramics, polymers, composites, and dissimilar materials have been successfully demonstrated.

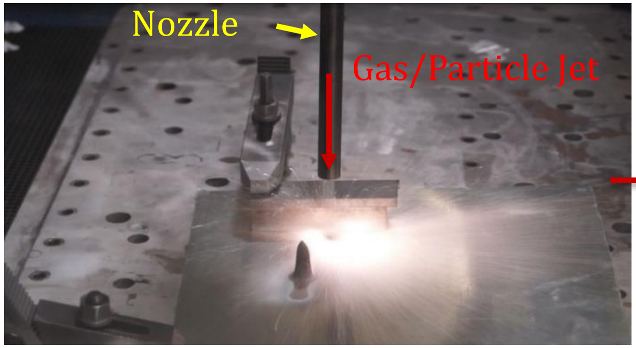

Spray Process

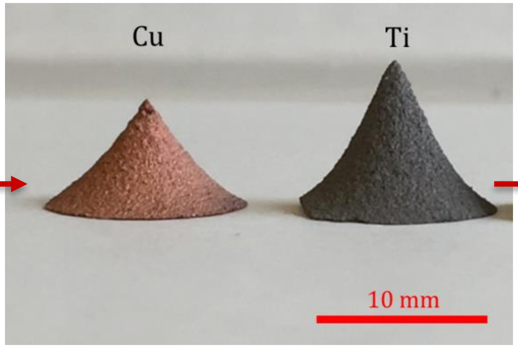

Deposition Process

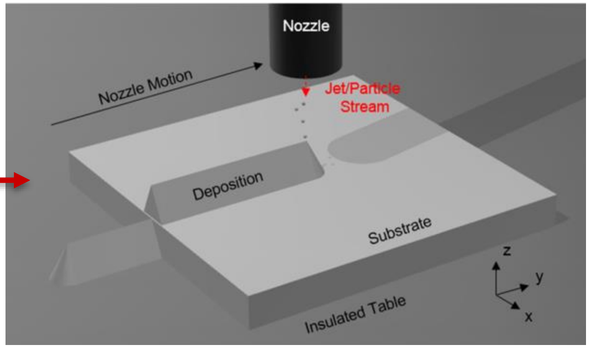

Building Process

Forms of Heat Addition in the CS Process

Supersonic Jet Impingement Heat Transfer

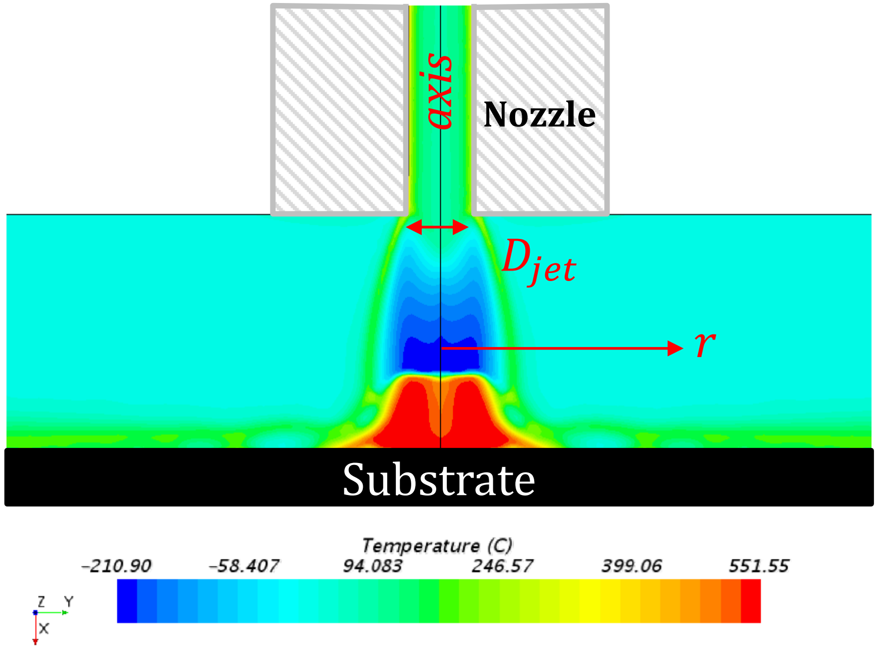

Heat Generation Due to Particle Impact

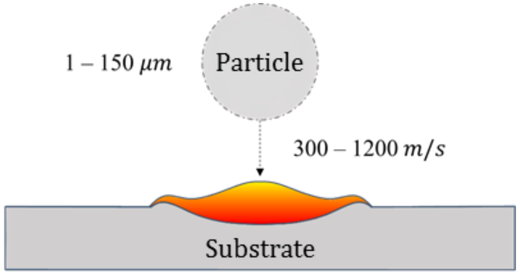

Retained Thermal Energy in the Deposited Material

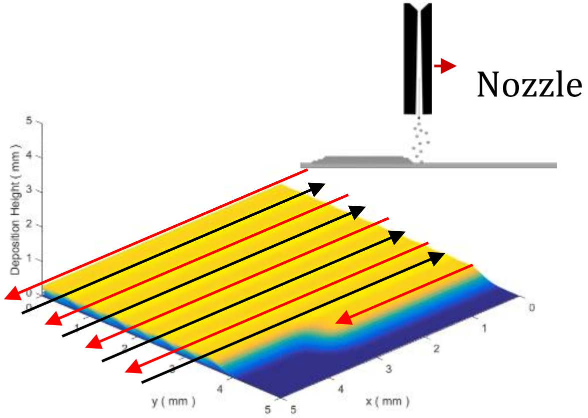

Necessity of Understanding Thermal History in CS

Importance

- Process control
- Product homogeneity
- Repeatability
- Understanding the resultant products properties
- Understanding needs for post processing (heat treatment)

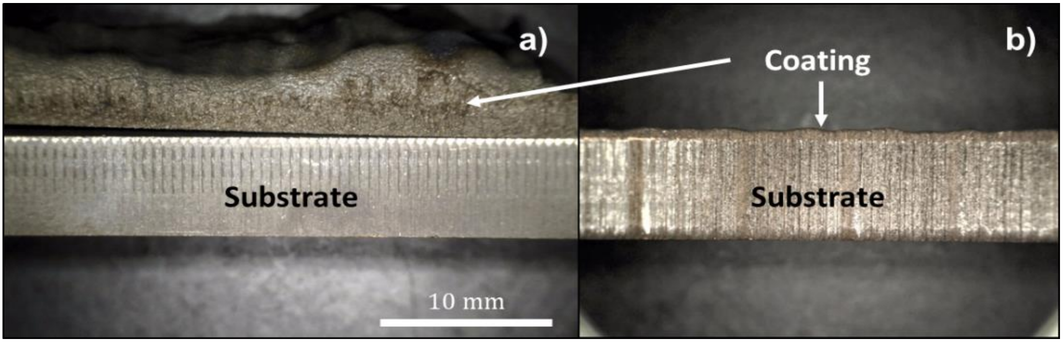

Ozdemir, O. C., *et al.*, "Predicting the Effects of Powder Feeding Rates on Particle Impact Conditions and Cold Spray Deposited Coatings," *Journal of Thermal Spray Technology*, Vol. 26, No. 7 (2017), pp. 1598-1615.

Examples

- Thermally sensitive applications (thin panel coating and repair, electronics, substrates with low melting temperatures)
- Incompatibilities in the powder/substrate coefficients of thermal expansion
- Understanding the potential thermal implications in failures like coating delamination

a) Delamination in thick layered coatings.
b) No delamination in thin layered coatings.

Does process thermodynamics have something to do with this?

Transient Thermal Simulation via Finite Volume Methods using Material Addition

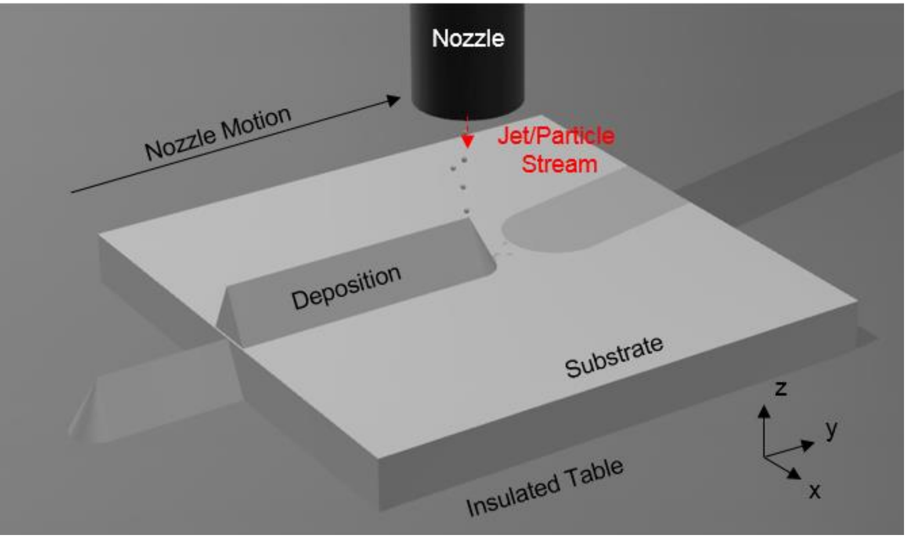

Computational Domain

m_m	Mass in cell
C_m	Material heat capacity
T	Temperature
t	Time
V	Volume
$\bar{q}$	Surface heat flux vector
S_{impact}	Volumetric heat generation due to particle impact

$$m_m\, C_m \frac{\partial T}{\partial t} = \underbrace{dV\left[-\nabla\bar{q} + \boldsymbol{S_{impact}}\right]}$$

Cell Heat Exchange Dynamics

- Heat Generation
  - Particle impact
- Thermal Energy of Added Mass
- Convection
  - Supersonic Jet Impingement
  - Surrounding Gas (Air)
- Conduction
  - Any solid-solid interactions of cells

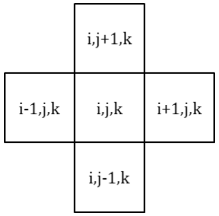

Quadrilateral cells

Jet Impingement Heat Transfer Properties via CFD

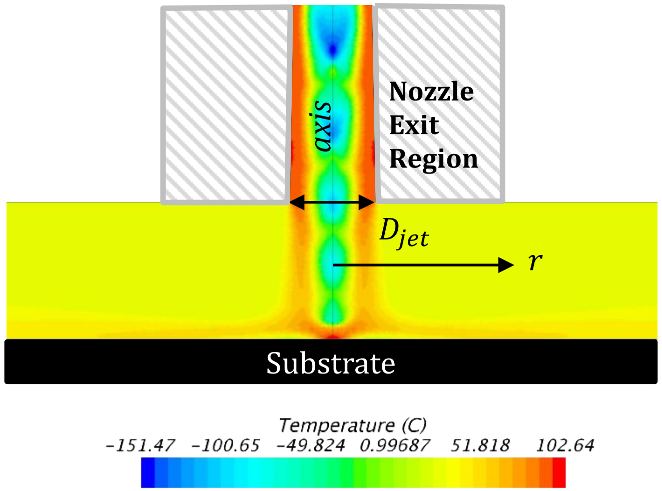

Validation heat transfer properties

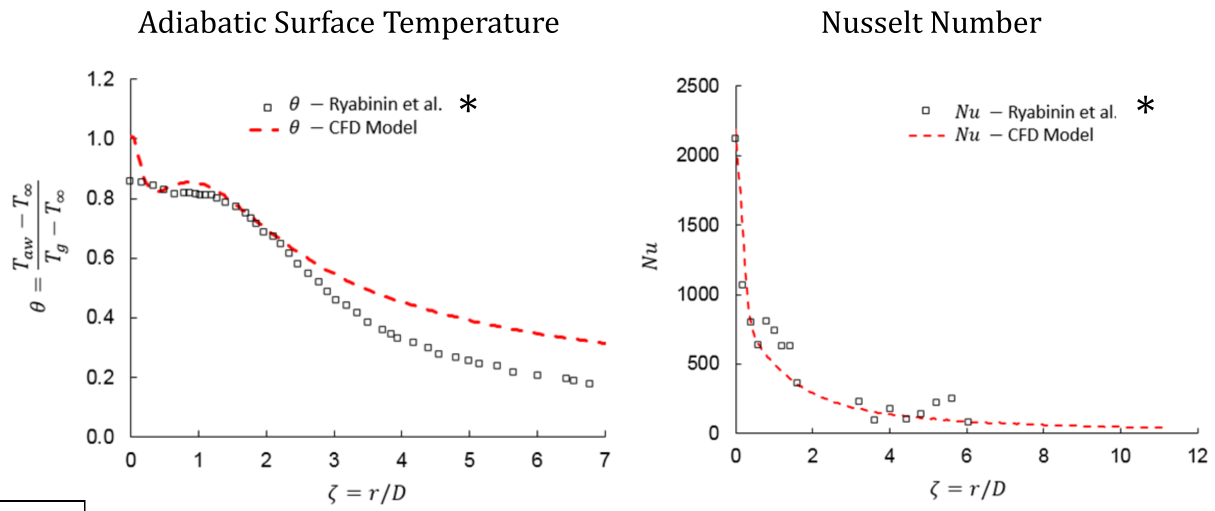
Adiabatic Surface Temperature

Nusselt Number

Nu_f	Nusselt number
k_f	Fluid thermal conductivity
D_{jet}	Characteristic length (jet diameter)
$\dot{q}_{conv}$	Conductive heat flux
h_f	Heat transfer coefficient
T_{aw}	Adiabatic substrate surface jet temperature
$T_{i,j,k}$	Exposed cell surface
A	Exposed cell surface area

$$h_f = \frac{k_f Nu_f}{D_{jet}} \qquad \dot{q}_{conv} = -h_f A (T_{ref} - T_{i,j,k})$$

* Ryabinin, A. N., *et al.*, "Simulation of gas-substrate heat exchange during cold-gas dynamic spraying," *International Journal of Thermal Sciences*, Vol. 56, (2012), pp. 12-18.

Heat Generation from Particle Impact Estimated from FEA

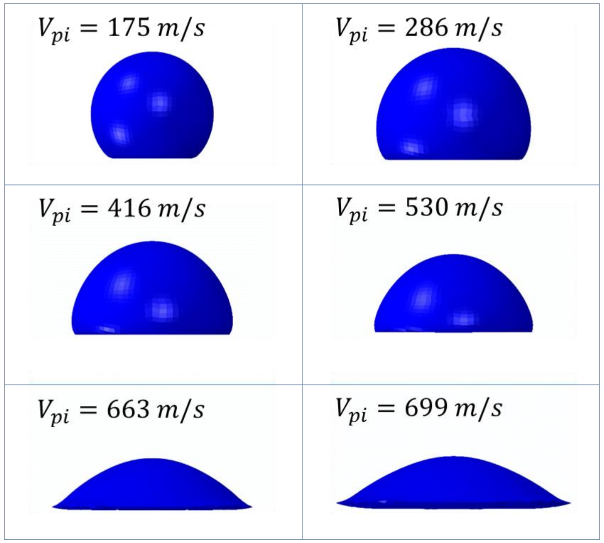

Q. Chen, A. Alizadeh, W. Xie, X. Wang, V. Champagne, A. Gouldstone, et al., "High-Strain-Rate Material Behavior and Adiabatic Material Instability in Impact of Micron-Scale Al-6061 Particles," Journal of Thermal Spray Technology, Vol. 27, No. 4 (2018), pp. 641-653.

K	Thermal energy conversion factor
b	Thermal softening factor
$\dot{m}_{in}$	Cell mass input rate
U_{pi}^2	Particle impact temperature

How much of the particle kinetic energy is converted into thermal energy?

$$m_m\, C_m \frac{\partial T}{\partial t} == -\sum \dot{\boldsymbol{q}}_{surf} + S_{impact}$$

$$S_{impact} = \left[K \frac{1}{2} \dot{m}_{in} U_{pi}^2\right] \left(1 - \frac{T_{i,j,k}^{t}{}' - T_{room}}{T_m - T_{room}}\right)^b$$

$K = 0.793$

90% of plastic energy is assumed to be converted into thermal energy.

$T_{i,j,k}^{t}{}'$	Particle-cell mass averaged initial cell temperature
T_m	Material melting temperature
T_{room}	Room temperature

Mass Addition

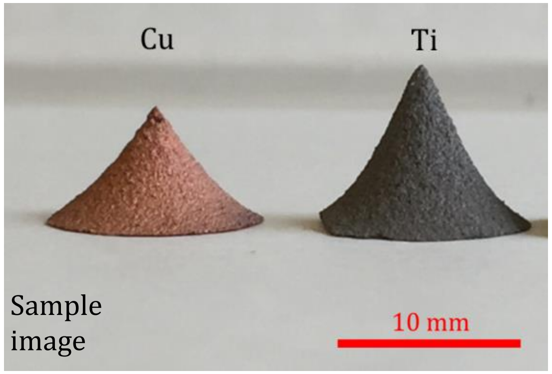

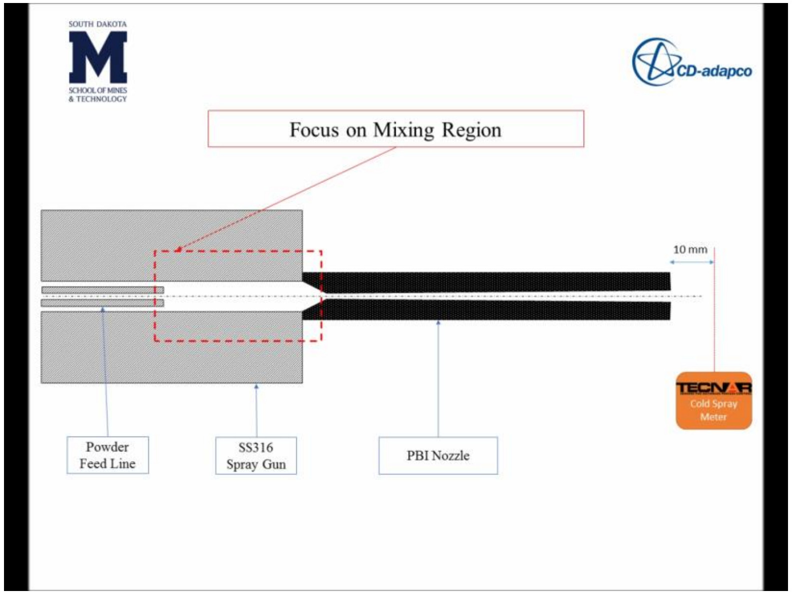

Ozdemir, O. C., *et al.*, "Influence of Powder Injection Parameters in High-Pressure Cold Spray," *Journal of Thermal Spray Technology*, Vol. 26, No. 7 (2017), pp. 1411-1422.

Mass flux in a cell is relative to its position from the nozzle axis.

2D Normal Distribution

$$\dot{m}'(\Delta x_N, \Delta y_N) = \dot{m}_{total}(C_1 - C_2)(C_3 - C_4)$$

$$C_1 = \frac{1}{2}\left(1 + \operatorname{erf}\left(\frac{\Delta x_N - \left(\mu_{mx} - \frac{1}{2}\Delta x\right)}{\sigma_{mx}\sqrt{2}}\right)\right)$$

$$C_2 = \frac{1}{2}\left(1 + \operatorname{erf}\left(\frac{\Delta x_N - \Delta x - \left(\mu_{mx} - \frac{1}{2}\Delta x\right)}{\sigma_{mx}\sqrt{2}}\right)\right)$$

$$C_3 = \frac{1}{2}\left(1 + \operatorname{erf}\left(\frac{\Delta y_N - \left(\mu_{my} - \frac{1}{2}\Delta y\right)}{\sigma_{my}\sqrt{2}}\right)\right)$$

$$C_4 = \frac{1}{2}\left(1 + \operatorname{erf}\left(\frac{\Delta y_N - \Delta y - \left(\mu_{my} - \frac{1}{2}\Delta y\right)}{\sigma_{my}\sqrt{2}}\right)\right)$$

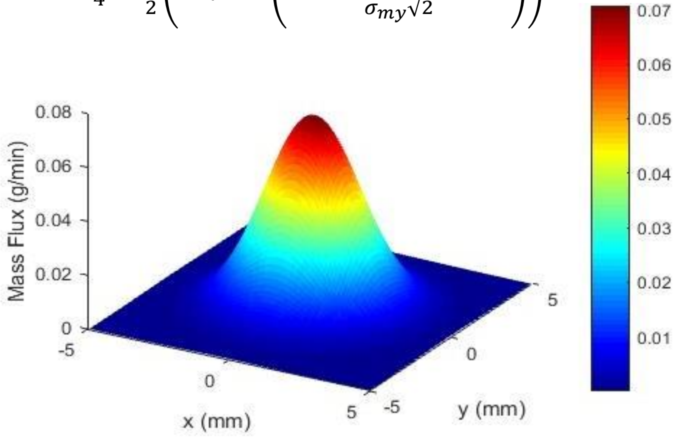

Mass flux distribution for 100 g/min deposition with $\mu_{mx} = \mu_{my} = 0\ mm$, $\sigma_{mx} = \sigma_{yx} = 1.5\ mm$, and $\Delta x = \Delta y = 0.1\ mm$.

Axisymmetric Cylindrical Model Adaptation

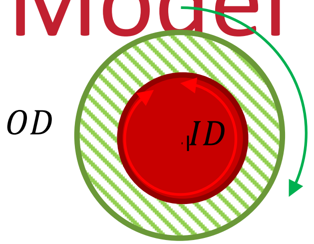

4. Heat loss to air from cylinder rotating about its axis.

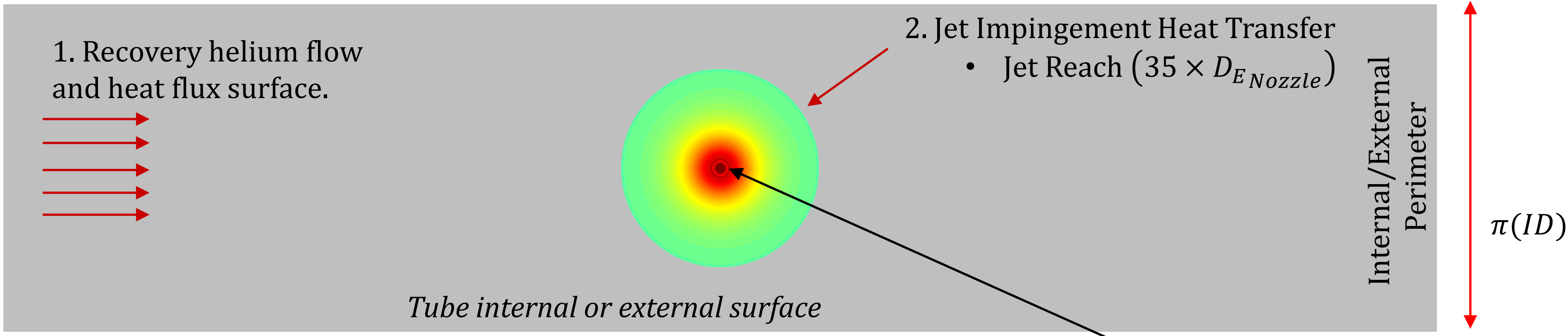

1. Recovery helium flow and heat flux surface.

2. Jet Impingement Heat Transfer
- Jet Reach $\left(35 \times D_{E_{Nozzle}}\right)$

3. Particle Impact Energy FEA simulations suggest 79.4% of the impact KE is converted to thermal energy.

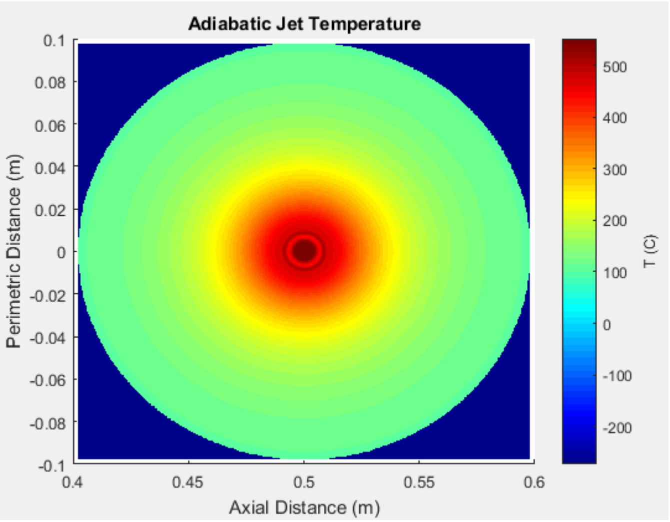

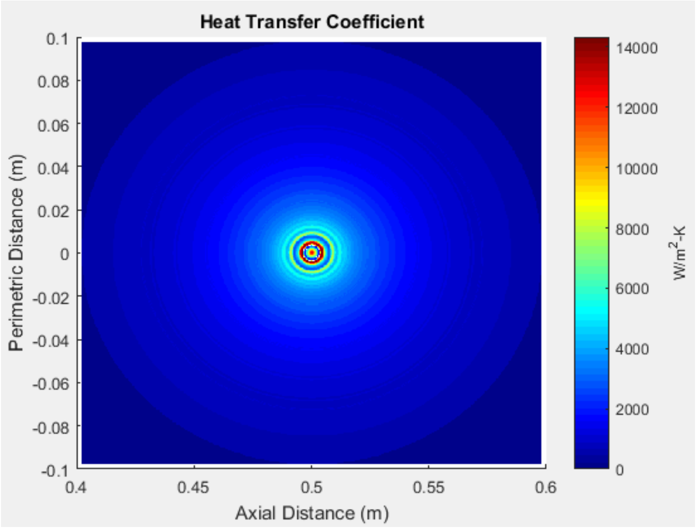

Conclusions

- A numerical tool for predicting heat generation in the cold spray process
- The tool that can be used for thermal control in CS
- Tool can also be used for added value to CS deposit property analysis.
- The model is also adapted as a 2D axisymmetric simulation to simplify cylindrical cases

Refer To:

Ozdemir, OC; Chen, Q.; Lin E.; Muftu, S. Modelling the Continuous Heat Generation in the Cold Spray Coating Process. Proceedings of the International Thermal Spray Conference. 2018 May 7-10; Orlando, FL. Materials Park: ASM International.

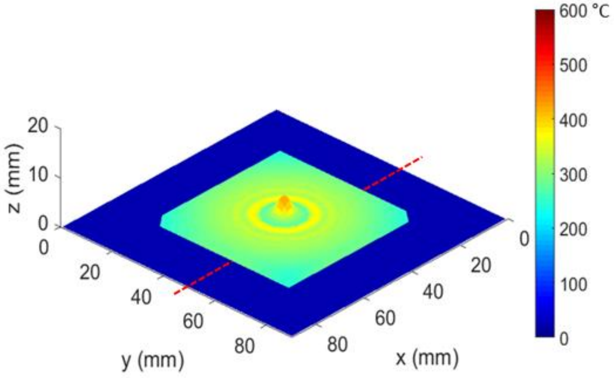

Questions

Acknowledgements

Further Questions?
Ozan Ozdemir
o.ozdemir@northeastern.edu

This work was sponsored in part by the U.S. Army Research Laboratories under the grant number W911NF-15-2-0026. Any opinions, findings and conclusions or recommendations expressed in this material are those of the author(s) and do not necessarily reflect the views of the U.S. Government.

Thank you

Northeastern University	Army Research Laboratory	United Technologies Research Center	VRC Metal Systems
Dr. Ozan Ozdemir Dr. Sinan Muftu Dr. Teiichi Ando Qiyong Chen Lauren Randaccio Tricia Schwartz	Vic Champagne Aaron Nardi	Dr. Matt Siopis	Kiley Plooster Kris Klus Terree Matson Rob Hrabe Robert Allegretto